

8-29-2009

High- K Multi-quasiparticle States and Rotational Bands in $^{255}_{103}\text{Lr}$.

H. B. Jeppesen

R. M. Clark

K. E. Gregorich

A. V. Afanasjev

M. N. Ali

*See next page for additional authors*Follow this and additional works at: <http://scholarship.richmond.edu/physics-faculty-publications> Part of the [Nuclear Commons](#)

Recommended Citation

Jeppesen, H. B., R. M. Clark, K. E. Gregorich, A. V. Afanasjev, M. N. Ali, J. M. Allmond, C. W. Beausang, M. Cromaz, M. A. Deleplanque, I. Dragojević, J. Dvorak, P. A. Ellison, P. Fallon, M. A. Garcia, J. M. Gates, S. Gros, I. Y. Lee, A. O. Macchiavelli, S. L. Nelson, H. Nitsche, L. Stavsetra, F. S. Stephens, and M. Wiedeking. "High- K Multi-quasiparticle States and Rotational Bands in $^{255}_{103}\text{Lr}$." *Physical Review C* 80, no. 3 (September 29, 2009): 034324: 1-34324: 4. doi:10.1103/PhysRevC.80.034324.

This Article is brought to you for free and open access by the Physics at UR Scholarship Repository. It has been accepted for inclusion in Physics Faculty Publications by an authorized administrator of UR Scholarship Repository. For more information, please contact scholarshiprepository@richmond.edu.

Authors

H. B. Jeppesen, R. M. Clark, K. E. Gregorich, A. V. Afanasjev, M. N. Ali, J. M. Allmond, C. W. Beausang, M. Cromaz, M. A. Deleplanque, I. Dragojevic, J. Dvorak, P. A. Ellison, P. Fallon, M. A. Garcia, J. M. Gates, S. Gros, I. Y. Lee, A. O. Macchiavelli, S. L. Nelson, H. Nitsche, L. Stavsetra, F. S. Stephens, and M. Wiedeking

High- K multi-quasiparticle states and rotational bands in $^{255}_{103}\text{Lr}$

H. B. Jeppesen,¹ R. M. Clark,¹ K. E. Gregorich,¹ A. V. Afanasjev,² M. N. Ali,^{1,3} J. M. Allmond,⁴ C. W. Beausang,⁴ M. Cromaz,¹ M. A. Deleplanque,¹ I. Dragojević,^{1,3} J. Dvorak,¹ P. A. Ellison,^{1,3} P. Fallon,¹ M. A. Garcia,^{1,3} J. M. Gates,^{1,3} S. Gros,¹ I. Y. Lee,¹ A. O. Macchiavelli,¹ S. L. Nelson,^{1,3} H. Nitsche,^{1,3} L. Stavsetra,¹ F. S. Stephens,¹ and M. Wiedeking¹

¹*Nuclear Science Division, Lawrence Berkeley National Laboratory, Berkeley, California 94720, USA*

²*Department of Physics and Astronomy, Mississippi State University, Mississippi 39762, USA*

³*Department of Chemistry, University of California, Berkeley, California 94720, USA*

⁴*Department of Physics, University of Richmond, Richmond, Virginia 23173, USA*

(Received 11 November 2008; published 29 September 2009)

Two isomeric states have been identified in ^{255}Lr . The decay of the isomers populates rotational structures. Comparison with macroscopic-microscopic calculations suggests that the lowest observed sequence is built upon the $[624]9/2^+$ Nilsson state. However, microscopic cranked relativistic Hartree-Bogoliubov (CRHB) calculations do not reproduce the moment of inertia within typical accuracy. This is a clear challenge to theories describing the heaviest elements.

DOI: [10.1103/PhysRevC.80.034324](https://doi.org/10.1103/PhysRevC.80.034324)

PACS number(s): 23.20.Lv, 21.10.Re, 27.90.+b, 29.30.Kv

I. INTRODUCTION

Super-heavy nuclei owe their existence to quantum shell structures arising from the bunching of single-particle levels; otherwise, they would immediately fission as a result of the massive Coulomb repulsion between protons. Theoretical models disagree on the single-particle structure and the location of shell gaps for these heaviest of nuclei (see Ref. [1] and references therein). To test the validity of the different predictions, the models can be compared against detailed spectroscopic information on nuclei with $Z > 100$, approaching the super-heavy region. In this paper, we report such a study on ^{255}Lr . We identify single- and multi-quasiparticle excitations and rotational bands. With 103 protons and 152 neutrons, this is the heaviest odd- Z nucleus for which such information is now available. We show that our new results challenge modern theories attempting to reproduce the properties and structures of the heaviest elements.

Of particular interest for this article is the study of multi-quasiparticle isomers, found in the region of prolate deformed nuclei near $Z \approx 100$ and $N \approx 152$. These nuclei have many high- K orbitals (where K is the projection of the total angular momentum on the symmetry axis) close to both the proton and neutron Fermi surfaces. This favors the occurrence of high- K multi-quasiparticle states at low excitation energy. Such states can become isomeric because of the approximate conservation of the K quantum number. Recently, detailed decay spectroscopy has been performed on K isomers in several nuclei with $Z \geq 100$, including ^{250}Fm [2], $^{252,254}\text{No}$ [3–5], and ^{256}Rf [6]. In this article, we report an investigation of K isomerism in ^{255}Lr ($Z = 103$). During the course of this work, a contemporaneous study of ^{255}Lr [7] reported the discovery of a high- K isomeric state with an estimated half-life of 1.4(1) ms and an excitation energy of $E_x > 720$ keV. The only other structure information on ^{255}Lr comes from α -decay studies [8,9] which associated the ground state with the $\pi[521]1/2^-$ Nilsson proton orbital and assigned an isomeric excited state at an excitation energy of ≈ 37 keV to the

$\pi[514]7/2^-$ orbital. Our results are much more extensive and include the observation of two high- K isomers, the decays of which allow us to define their excitation energies and to suggest spins and parities. Moreover, the decay of these isomers populates rotational structures; the first to be observed in any nucleus with $Z > 102$.

II. EXPERIMENTAL DETAILS

The experiment was performed at the 88-inch cyclotron of the Lawrence Berkeley National Laboratory and used the Berkeley gas-filled separator (BGS) [10]. The ^{255}Lr nuclei were produced in the $^{209}\text{Bi}(^{48}\text{Ca}, 2n)$ fusion-evaporation reaction at a beam energy of 222 MeV (around 219 MeV at the center of the target, corresponding to a cross section of ≈ 400 nb [11]). The ^{48}Ca beam from the 88-inch cyclotron passed through a $\approx 45 \mu\text{g}/\text{cm}^2$ carbon window (separating the He gas inside the BGS from the beamline vacuum) and was incident on ^{209}Bi targets of $\approx 0.4 \text{ mg}/\text{cm}^2$ thickness, each with a $\approx 35 \mu\text{g}/\text{cm}^2$ carbon backing. The targets were mounted on a rotating target wheel. The average beam intensity for the 5 day run was about 200 pA. Evaporation residues were separated from the beam and other reaction products by their differing magnetic rigidities, and then passed through a multi-wire proportional counter (MWPC), before being implanted in a 1 mm thick 16×16 double-sided silicon strip detector (DSSSD) with an active area of 5×5 cm. A standard clover Ge detector [12] was mounted behind the 2 mm Al backplate of the BGS focal plane at approximately 5 mm from the DSSSD. Standard γ -ray sources of ^{207}Bi , ^{152}Eu , and ^{241}Am were used for energy and efficiency calibrations. We reproduced the focal plane distribution of recoils by performing source measurements over the surface of the DSSSD, which yielded an absolute photopeak efficiency of $\approx 17\%$ at 122 keV and $\approx 3.5\%$ at 1 MeV. In the analysis described below, all the γ -ray spectra were created by treating the four clover Ge crystals as individual detectors (no addback).

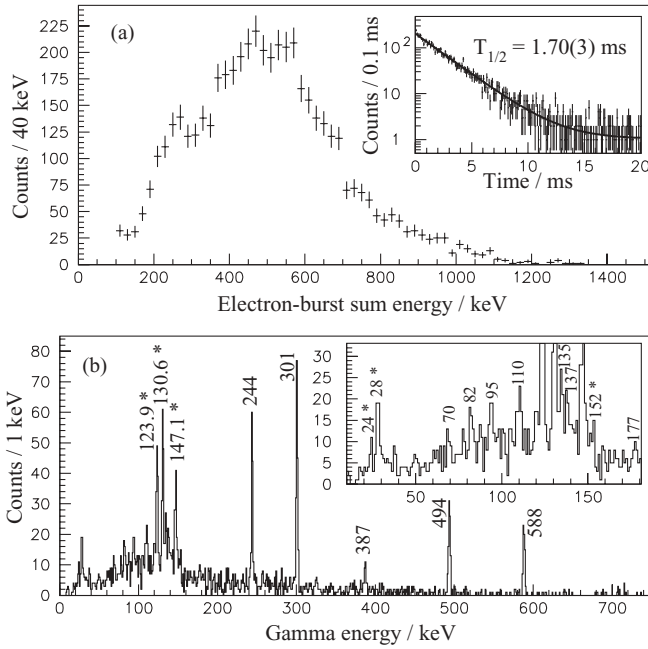


FIG. 1. (a) Electron-burst sum energy for all r - e events. The insert shows the time difference between each electron burst and the associated recoil. (b) γ rays in coincidence with the electron bursts. The insert shows an expansion of the low-energy part of the spectrum. Asterisks indicate known Lr X rays.

III. RESULTS

Recoils were identified by a MWPC signal in coincidence with an implant in a DSSSD pixel. During the experiment, a total of 5.9×10^4 recoil implants were recorded, and out of those, 2.2×10^4 were followed by an α decay, in the same pixel, characteristic of ^{255}Lr (denoted as r - α events). Our analysis of the α decays agrees with prior measurements [8,9] and indicates that essentially all the detected recoils are ^{255}Lr ions.

To identify isomeric electromagnetic decays, we searched for a delayed electron signal, within the same pixel of the DSSSD as an implanted recoil [13]. A total of 4.9×10^3 such electron bursts was recorded following a recoil implant (r - e events), indicating the presence of an isomer. Figure 1(a) shows the energy distribution of the electron bursts within 10 ms of the recoil implant. The insert shows the time difference between recoil implants and the subsequent electron burst. The line represents a best fit to the data using an exponential decay plus a constant background, yielding a half-life of 1.70(3) ms for the isomeric state. From r - e - α events (r - e events followed by an α decay), we determine that the isomer decays predominantly to the known excited state at ≈ 37 keV, which then decays via α decay or internal conversion. Figure 1(b) shows the γ -ray spectrum obtained in prompt coincidence with the electron bursts. X rays known to come from ^{255}Lr (marked with an asterisk) are seen, along with several prominent γ lines which we attribute to ^{255}Lr . The insert in Fig. 1(b) shows an expansion of the low-energy part of the γ -ray spectrum.

In Table I, we present the energies and relative intensities of the γ rays which we are able to identify from the γ -ray spectrum [Fig. 1(b)]. From the well-known K X-ray relative

TABLE I. Transition energies E_γ (in keV), relative intensities corrected for detector efficiency I_γ (normalized to the 494 keV transition), spin-parity assignment of initial and final states, and the total relative intensity I_{tot} (after correction of internal conversion) of the γ -ray transitions assigned to ^{255}Lr .

E_γ	I_γ	Assignment	I_{tot}
69.5(4)	0.10(4)	$(11/2^+) \rightarrow (9/2^+)$	4.2(17)
82.3(3)	0.16(5)	$(13/2^+) \rightarrow (11/2^+)$	4.3(13)
94.7(3)	0.18(4)	$(15/2^+) \rightarrow (13/2^+)$	3.3(8)
110.4(3)	0.19(4)	$(17/2^+) \rightarrow (15/2^+)$	2.3(5)
123(1) ^a	0.13(4)	$(19/2^+) \rightarrow (17/2^+)$	1.2(4)
135.2(3)	0.22(4)	$(21/2^+) \rightarrow (19/2^+)$	1.6(3)
137.4(4)	0.18(4)	$(21/2^-) \rightarrow (19/2^-)$	1.2(3)
148.3(4) ^b	0.25(6)	$(23/2^-) \rightarrow (21/2^-)$	1.4(3)
177.0(4)	0.06(2)	$(15/2^+) \rightarrow (11/2^+)$	0.2(1)
243.9(3)	0.73(11)	$(25/2^+) \rightarrow (23/2^-)$	0.8(1)
300.6(3)	1.20(14)	$(25/2^+) \rightarrow (21/2^+)$	1.6(2)
386.6(4)	0.23(8)	$(15/2^+) \rightarrow (17/2^+)$	0.5(2)
493.5(3)	1.00(14)	$(15/2^+) \rightarrow (15/2^+)$	1.7(2)
588.1(3)	0.91(15)	$(15/2^+) \rightarrow (13/2^+)$	1.3(2)

^aUnderneath $K_{\alpha 2}$ X ray.

^bNear $K_{\beta 1}$ X ray.

intensities, we are able to infer the presence of unresolved γ -ray transitions at 123 keV (on the low energy side of the $K_{\alpha 2}$ X ray) and 148 keV (on the high energy side of the $K_{\beta 1}$ X ray). In Table I, the relative intensities of all the γ -ray transitions, after correction for detection efficiency, are normalized to the intensity of the 494 keV transition. Figure 2 shows our proposed decay scheme. The assignments and relative total intensities, after correction for internal conversion [14], are also given in Table I. It should be noted that we have assumed a pure character for all the transitions. Also, we see several weak transitions including 258, 324, and 707 keV [see Fig. 1(b)], which may indicate additional, weaker, parallel pathways depopulating the millisecond isomer.

Most of the low-energy γ rays are assigned as $M1$ transitions depopulating rotational states. In making spin

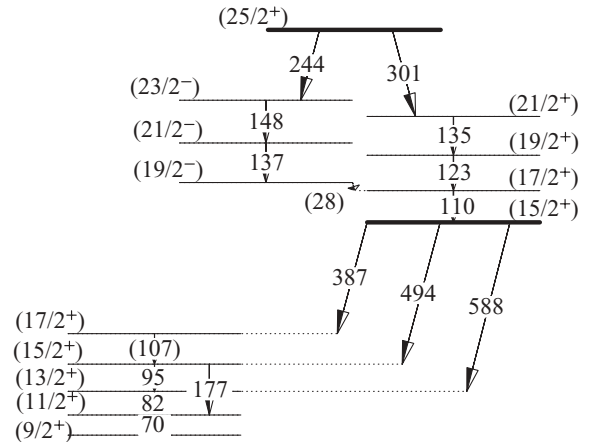


FIG. 2. Level scheme for ^{255}Lr . Energies are in keV. Suggested spins and parities are indicated in parentheses. The two isomeric states are indicated by thicker lines.

assignments, we require consistency with the transition energies of the rotational bands known in the lighter actinides. From the observed total energy of the isomer decay, the bandhead of the lowest rotational band must be within ~ 100 keV of the ground state.

The high-energy transitions have been placed on the basis of their energy sums, intensity balances, and γ - γ correlations. The 387, 494, and 588 keV lines are parallel (confirmed by the γ - γ coincidences) and feed into the lowest rotational sequence. They are assigned as $M1$ transitions. These three transitions show a time delay relative to the 244 and 301 keV lines, and we infer that the intermediate state is also isomeric with an estimated half-life of several tens of nanoseconds. This is much shorter than the flight time of recoils through the BGS (≈ 1 μ s), and this state must be populated following the decay of the highest isomer. The 244 and 301 keV transitions depopulate the 1.70(3) ms isomer, and γ - γ correlations confirm that they feed parallel paths. Intensity from both paths feeds into the 110 keV $M1$ transition, and we infer the presence of a 28 keV $E1$ transition as shown in Fig. 2. This is the same energy as the $L_{\gamma 1}$ X ray in ^{255}Lr , which is clearly seen in Fig. 1(b). We also see the $L_{\beta 1}$ X ray at 24 keV. At these small γ -ray energies, it is very difficult to measure accurately the relative efficiency, but we estimate that the 28 keV line has a significantly larger intensity than expected relative to the 24 keV line. Therefore, we propose the 28 keV transition, which must be of $E1$ character to be seen in the spectrum. The state depopulated by this 28 keV $E1$ transition may also be long-lived (≥ 10 ns based on an estimate of the $E1$ hindrance). Consistency with the spin-parity assignments of lower lying states suggests that the 244 keV transition is of $E1$ character and the 301 keV transition is an $E2$.

IV. DISCUSSION

We now compare the data with various theoretical predictions. Note, these models all give different predictions for the location and size of the major spherical shell gaps responsible for the existence of the super-heavy elements. By comparing them with our results, we are testing the ability of the different models to reproduce the single-particle structure of the heaviest odd- Z system studied in detail to date. There are prior calculations of the low-lying level structure of ^{255}Lr from a macroscopic-microscopic (MM) approach based on the Nilsson-Strutinsky method with a Woods-Saxon potential [15], and a nonrelativistic Hartree-Fock Bogoliubov calculation with the Skyrme SLy4 interaction (HFB-SLy4) [16]. In addition, we have performed cranked relativistic Hartree-Bogoliubov (CRHB) calculations employing the NL1 and NL3 parametrizations of the relativistic mean-field (RMF) Lagrangian for the particle-hole channel and with the D1S Gogny force for the particle-particle channel. Details of the formalism can be found in Ref. [17]. Results from these theoretical approaches are compared with experiment in Fig. 3.

The MM calculations predict three closely spaced one-quasiproton states below an excitation energy E_x of 150 keV. Using the Nilsson labels, they are $[514]7/2^-$, $[624]9/2^+$, and

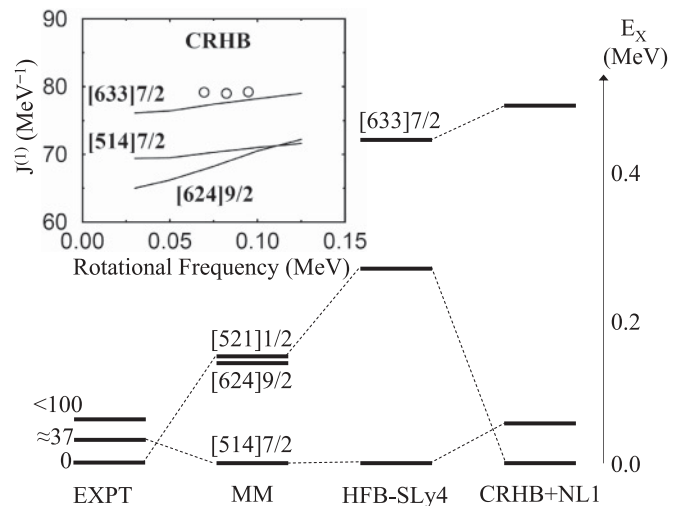


FIG. 3. Experimental (energies in keV) and calculated (with Nilsson labels) one-quasiproton states in ^{255}Lr . The notations MM, HFB-SLy4, and CRHB + NL1 label the respective calculations. The inset shows kinematic moments of inertia from CRHB calculations (solid lines) and experiment (open circles).

$[521]1/2^-$. The MM calculations provide the best current description of the one-quasiparticle energies in the lower- Z actinides (generally reproduced to within 200 keV), and we would expect such calculations to accurately reflect the low-lying level structure of ^{255}Lr .

The HFB-SLy4 and CRHB + NL1 calculations also predict that the $[514]7/2^-$ and $[521]1/2^-$ are low-lying levels but place the $[624]9/2^+$ state at a high excitation energy ($E_x > 800$ keV). The $[633]7/2^+$ state is predicted to lie closer to the ground state at around $E_x \approx 400$ keV. The $[633]7/2^+$ and $[624]9/2^+$ states arise from the same $i_{13/2}$ spherical subshell. It has been noted that the relative energy of the $i_{13/2}$ subshell with respect to other subshells can differ from experiment by several hundred keV in self-consistent calculations [16,17]. The $[633]7/2^+$ Nilsson state is known to be the ground state in several Bk isotopes ($Z = 97$) including the $N = 152$ isotone, ^{249}Bk [18]. Empirically, it seems unreasonable that this state is also within ~ 100 keV of the ground state in ^{255}Lr ($Z = 103$).

The low-lying band is not based on the $[521]1/2^-$ ground state, since one would expect a decoupled structure similar to that seen in ^{251}Md [19]. The $[514]7/2^-$ and $[624]9/2^+$ states have different gyromagnetic factors g_K , which will be reflected in the relative strengths of the intraband $M1$ and $E2$ transitions. We see a 177 keV transition which we assign as an $E2$ cross-over transition (see Figs. 1 and 2). From the relative intensities of the 95 keV $M1$ transition and the 177 keV $E2$ transition, we find a value of $B(M1)/B(E2) = 0.45(18)$ ($\mu_N/e b$) 2 . Assuming the quadrupole deformation of the band to be $\beta_2 = 0.3$ (typical for nuclei in this region), estimates of the $B(M1)/B(E2)$ values for the $[514]7/2^-$ and $[624]9/2^+$ states are 0.03 and 0.64 ($\mu_N/e b$) 2 , respectively. Between these two Nilsson states, we favor the $[624]9/2^+$ assignment. [Note, for the $[633]7/2^+$ level, we estimate a value of $B(M1)/B(E2) \approx 0.3$ ($\mu_N/e b$) 2 and cannot exclude it solely on the basis of the experimental $B(M1)/B(E2)$ ratio]. It

is unclear if this means that the first excited state, assumed to be the $[514]7/2^-$ state, has been misassigned or if the rotational band is built upon the $[624]9/2^+$ state above the $[514]7/2^-$ state. In the latter case, the two states would be connected by a prompt $E1$ transition. No such γ line is observed, and the energy difference between the $[624]9/2^+$ and $[514]7/2^-$ states must be small (<30 keV).

We used the CRHB approach to calculate moments of inertia for bands based on the different one-quasiparticle states. The results are shown in the inset of Fig. 3. If our $[624]9/2^+$ assignment is correct, then the discrepancy with the CRHB calculation is much larger than is typical [17]. Indeed, we performed calculations on ^{251}Es ($Z = 99$, $N = 152$) and reproduced the moments of inertia for the assigned $[633]7/2^+$ and $[624]9/2^+$ bands [20] to within 7% accuracy. On the basis of the moment of inertia, the CRHB calculation would favor the $[633]7/2^+$ assignment. This illustrates the importance of our data as a test of theory. Either the single-particle prediction of the MM model or the moment of inertia from the CRHB calculation are far outside the typical expected uncertainty. Significant alteration of the single-particle structure from the MM model does not seem possible without upsetting the agreement with data on lighter actinides.

While the spins of the states are generally fixed by our earlier arguments of energy spacings, multipole character of transitions, and decay paths, the assignment of the low-lying rotational band to the $[624]9/2^+$ orbital yields probable parities. The intermediate isomeric state has the most likely spin-parity assignment of $I^\pi = 15/2^+$, while the higher lying isomer is most likely $I^\pi = 25/2^+$. The spins and excitation energies of these isomeric states suggest that they are three-quasiparticle high- K states. We can estimate the hindrance factors of K -forbidden transitions from these states. The hindrance factor F_W is given by the expression $F_W = [(t_{1/2})_{\text{exp}}/(t_{1/2})_{\text{WU}}]$, where $(t_{1/2})_{\text{exp}}$ is the partial γ -ray half-life and $(t_{1/2})_{\text{WU}}$ is the Weisskopf estimate. The three $\Delta K = 3$ $M1$ transitions depopulating the $15/2^+$ state, and the 244 keV $\Delta K = 3$ $E1$ transition and 301 keV $\Delta K = 5$ $E2$ transition from the $25/2^+$ state, have hindrance factors consistent with the systematics of Löbner [21], lending further support to the proposed level scheme.

To assign configurations to the observed three-quasiparticle states, one must consider high- K orbitals near to both the proton and neutron Fermi surfaces. As discussed above, active high- K proton orbitals include the $[514]7/2^-$ and $[624]9/2^+$ Nilsson levels. Active high- K neutron orbitals include the $[734]9/2^-$, $[613]7/2^+$, $[624]7/2^+$, and $[725]11/2^-$ orbitals. It seems likely that the $K^\pi = 15/2^+$ state is based on the $\pi(\downarrow[521]1/2^- \otimes \uparrow[514]7/2^- \otimes \uparrow[624]9/2^+)_{K=15/2}$ three-quasiproton configuration, which is formed from the three lowest one-quasiproton excitations. Note, the $\pi(\downarrow[521]1/2^- \otimes \uparrow[514]7/2^-)$ configuration is assigned as the configuration of a low-lying $K^\pi = 3^+$ level in ^{254}No [5]. To form the $K^\pi = 25/2^+$ state, it seems likely that a single-quasiproton state is coupled to a two-quasineutron configuration. A possible configuration is $\pi[514]7/2^- \otimes \nu([725]11/2^- \otimes [624]7/2^+)$. It will be interesting to examine the properties of the bands based on these high- K configurations, both theoretically and experimentally, to test the configuration assignments.

V. SUMMARY

In summary, two high- K three-quasiparticle isomers have been found in ^{255}Lr . The decay of the isomers populates rotational bands. Comparison with MM calculations suggest that the lowest band is based on the $\pi[624]9/2^+$ Nilsson proton state. However, microscopic CRHB calculations do not reproduce the moment of inertia of this assignment within typical accuracy. Our results represent a clear challenge to theories describing the structure and properties of the heaviest elements.

ACKNOWLEDGMENTS

We thank the staff of the 88-inch cyclotron. R.M.C. thanks T. J. Smith for her help. This work was supported in part by the US DOE under Contract No. DE-CA02-05CH11231 (LBNL) and Grant Nos. DE-FG52-06NA26206, DE-FG02-05ER41379, and DE-FG02-07ER41459.

-
- [1] Y. Oganessian, *J. Phys. G* **34**, R165 (2007).
 - [2] P. T. Greenlees *et al.*, *Phys. Rev. C* **78**, 021303(R) (2008).
 - [3] B. Sulignano *et al.*, *Eur. Phys. J. A* **33**, 327 (2007).
 - [4] S. K. Tandel *et al.*, *Phys. Rev. Lett.* **97**, 082502 (2006).
 - [5] R.-D. Herzberg *et al.*, *Nature* **442**, 896 (2006).
 - [6] H. B. Jeppesen *et al.*, *Phys. Rev. C* **79**, 031303(R) (2009).
 - [7] K. Hauschild *et al.*, *Phys. Rev. C* **78**, 021302(R) (2008).
 - [8] A. Chatillon *et al.*, *Eur. Phys. J. A* **30**, 397 (2006).
 - [9] F. P. Hessberger *et al.*, *Eur. Phys. J. A* **29**, 165 (2006).
 - [10] C. M. Folden III, Ph.D. thesis, University of California, Berkeley, Report No. LBNL-56749, 2004.
 - [11] H. W. Gäggeler *et al.*, *Nucl. Phys.* **A502**, 561c (1989).
 - [12] G. Duchêne *et al.*, *Nucl. Instrum. Methods A* **432**, 90 (1999).
 - [13] G. D. Jones, *Nucl. Instrum. Methods A* **488**, 471 (2002).
 - [14] T. Kibédi *et al.*, *Nucl. Instrum. Methods A* **589**, 202 (2008).
 - [15] S. Ćwiok, S. Hofmann, and W. Nazarewicz, *Nucl. Phys.* **A573**, 356 (1994).
 - [16] M. Bender *et al.*, *Nucl. Phys.* **A723**, 354 (2003).
 - [17] A. V. Afanasjev, T. L. Khoo, S. Frauendorf, G. A. Lalazissis, and I. Ahmad, *Phys. Rev. C* **67**, 024309 (2003).
 - [18] I. Ahmad *et al.*, *Phys. Rev. C* **71**, 054305 (2005).
 - [19] A. Chatillon *et al.*, *Phys. Rev. Lett.* **98**, 132503 (2007).
 - [20] J. K. Tuli, S. Singh, and A. K. Singh, *Nucl. Data Sheets* **107**, 1347 (2006).
 - [21] K. E. G. Löbner, *Phys. Lett.* **B26**, 369 (1968).